Transitions in a self-propelled-particles model with coupling of accelerations

Péter Szabó*
Department of Biological Physics, Eötvös University, Pázmány P. sétány. 1A, H-1117 Budapest, Hungary
and Department of Ecology, Faculty of Veterinary Science, Szent István University, Rottenbiller u. 50, H-1077 Budapest, Hungary

Máté Nagy†
Department of Biological Physics, Eötvös University, Pázmány P. sétány. 1A, H-1117 Budapest, Hungary

Tamás Vicsek‡
Department of Biological Physics, Eötvös University, Pázmány P. sétány. 1A, H-1117 Budapest, Hungary
and Biological Physics Research Group of HAS, Pázmány P. sétány. 1A, H-1117 Budapest, Hungary
(Received 29 July 2008; published 10 February 2009)

We consider a three-dimensional, generalized version of the original self-propelled-particles (SPP) model for collective motion. By extending the factors influencing the ordering, we investigate the case when the movement of the SPPs depends on both the velocity and the acceleration of the neighboring particles, instead of being determined solely by the former one. By changing the value of a weight parameter s determining the relative influence of the velocity and the acceleration terms, the system undergoes a kinetic phase transition as a function of a behavioral pattern. Below a critical value of s the system exhibits disordered motion, while above it the dynamics resembles that of the SPP model. We show that the critical value of the strategy variable could correspond to an evolutionary optimum in the sense that the information exchange between the units of the system is maximal in this point.

DOI: 10.1103/PhysRevE.79.021908 PACS number(s): 87.15.Zg, 87.19.lo

I. INTRODUCTION

Collective motion of organisms (e.g., fish schools, bird flocks, bacterial colonies) exhibits a large variety of emergent phenomena [1–8]. Synchronized motion, symmetrical group formations (e.g., V shaped), or swirling patterns emerge in spite of the apparently simple behavioral rules of the individual flock members [9–14]. The self-propelled-particles (SPP) model was proposed by Vicsek *et al.* [15] to describe the onset of ordered motion within a group of self-propelled particles in the presence of perturbations. Taking into account the effects of fluctuations inevitably present in biological systems was an essential generalization of the previously deterministic flocking models such as that of Reynolds [16]. The original model considers pointlike particles moving at constant velocity on a two-dimensional surface with periodic boundary conditions. The only rule is that at each time step every particle approximate, with some uncertainty, the average direction of motion of the particles within its neighborhood of radius R. This model exhibits spontaneous self-organization; by decreasing the noise parameter, the system undergoes a kinetic phase transition from a disordered state to an ordered one where all the particles move approximately in the same direction. Due to its simplicity and analogy with biological systems comprised of many, locally interacting units, the SPP model has emerged as a widely used model for phase-transition-like ordering in systems exhibiting flockinglike behavior [17–27].

The individually based behavioral rules determining collective motion are of particular interest. Important elements of these behavioral rules are the nature of the perceived information and the affected behavioral traits [28–30]. A frequent assumption in models is that the information perceived by the particles is restricted to the velocity and the relative distance of their neighbors. The interaction range is usually defined by metric distances, but Ballerini *et al.* [28] recently showed that topological distance may be the one factor determining the flocking of starlings. The assumption that particles react only to momentary behavioral clues may not describe a number of biologically relevant situations adequately. We expect that the behavior of the SPP model will be significantly extended if we also incorporate a term corresponding to memory on short time scales. This can be achieved by introducing an acceleration term into the equations. This is equivalent to separating the time scales by assuming that the particles differentiate between two kind of information: their actual velocity and the recent change in their direction of motion. For example, in the case of birds, reacting to acceleration may mean that birds can give signals to their neighbors about their intended flight maneuvers by quickly modifying their direction of motion.

The reasons behind particular manifestations of collective motion patterns are only partially understood. It seems that, for example, the various interpretations of the V-shaped formations displayed by large migrating birds still remain after several decades of possible explanations (see, e.g., [31,32]). Patterns of collective motion involving sharp turns of the whole flock still represent a beautiful challenge. Observations of rock doves [33] and starlings (see, e.g., [28]) suggest a rich interaction of birds within the flocks such that they seem to be capable of adopting the same direction of motion within a tiny fraction of a second.

*pszabo@angel.elte.hu
†nagymate@angel.elte.hu
‡vicsek@angel.elte.hu

II. MODEL

In the three-dimensional, scalar noise (SNM) version [34] of the original SPP model [15], the particles are assumed to move with a constant velocity v and their positions are updated simultaneously according to

$$\mathbf{x}_i(t+\Delta t) = \mathbf{x}_i(t) + \mathbf{v}_i(t)\Delta t, \tag{1}$$

where $\mathbf{x}_i$ and $\mathbf{v}_i$ are position and velocity of particle i, respectively. The time increment is set to be $\Delta t=1$. Each particle is assumed to move, with some uncertainty, in the average direction of all the particles within a fixed neighborhood of radius $R=1$. Hence the new velocity is given by

$$\mathbf{v}_i(t+\Delta t) = v \cdot \mathcal{M}(\mathbf{e},\xi) \cdot \mathbf{N}(\langle \mathbf{v}(t)\rangle_{i,R}), \tag{2}$$

where v is the absolute value of velocity, $\mathcal{M}(\mathbf{e},\xi)$ is a rotational tensor representing a random perturbation, $\langle \mathbf{v}(t)\rangle_{i,R}$ denotes the average velocity of all particles around particle i within radius R including particle i itself, and $\mathbf{N}(\mathbf{u})=\mathbf{u}/|\mathbf{u}|$. $\mathcal{M}(\mathbf{e},\xi)$ performs a rotation of angle ξ around a vector $\mathbf{e}$; ξ is a uniform random value in the interval $[-\eta\pi,\eta\pi]$, whereas $\mathbf{e}$ is a random unit vector chosen uniformly from the set of vectors perpendicular to $\mathbf{N}(\langle \mathbf{v}(t)\rangle_{i,R})$. The order in which (1) and (2) are calculated has some quantitative effects on the results (see later).

Here we introduce the acceleration-coupled SPP (AC-SPP) model, being a modified version of the SNM, in which the velocity vector $\mathbf{v}_i(t+\Delta t)$ is a function of both the velocity $\mathbf{v}(t)$ and the acceleration $\mathbf{a}(t)=[\mathbf{v}(t)-\mathbf{v}(t-\Delta t)]/\Delta t$ of the neighboring particles. Then Eq. (2) becomes

$$\mathbf{v}_i(t+\Delta t) = v \cdot \mathcal{M}(\mathbf{e},\xi) \cdot \mathbf{N}(s \cdot \langle \mathbf{v}(t)\rangle_{i,R} + (1-s) \cdot \langle \mathbf{a}(t)\Delta t\rangle_{i,R}), \tag{3}$$

where $s \in (0,1]$ is a so-called strategy parameter expressing the relative influence of the acceleration and velocity tags on the velocity vector of the focal particle. The acceleration term is calculated for every particle separately. In Eq. (3) we average this quantity for only those particles which are within a range of radius R of the ith particle in time step t (including particle i itself). Initially we have $N=\rho L^3$ randomly distributed particles, where L and ρ stand for box size and particle number density, respectively. The bounding box has periodic boundary conditions. The velocity parameter used in the simulations is $v=0.1$, corresponding to the low-velocity regime [25].

Taking into account the acceleration in a separate term has various possible functions. As for the contribution of the ith particle, it corresponds to a memory effect: a given particle, if it has no neighbors, has a tendency to keep on turning as it did in the previous time step (see also [30]). Perhaps more importantly, the average turning rate of the neighbors has now a separated effect on the turning rate of the ith particle. In the limit where is s close to 1, the AC-SPP model is very much like the original SPP model, while for $s \ll 1$ the acceleration term dominates and instantaneous turning of the neighbors has a strong effect on the trajectory of the ith particle. We quite naturally assume that the velocity can be associated with the actual "state" of a particle. Acceleration is already a derivative (both literally and on general terms) of the state and can be looked at as a separate feature influencing the state of a particle. For example, in the case of birds, we assume that the degree to which birds reflect upon the changing of the flight direction of the other birds nearby can be separated from the shear tendency to follow the neighbors. We say that being sensitive (e.g., overreacting) to directional changes is a different behavioral pattern from not paying extra attention to this aspect of the motion. We associate, for example, with such a behavioral pattern a short turning period of a bird flying in a flock and giving signs for its neighbors of its intended changing of the direction of flight.

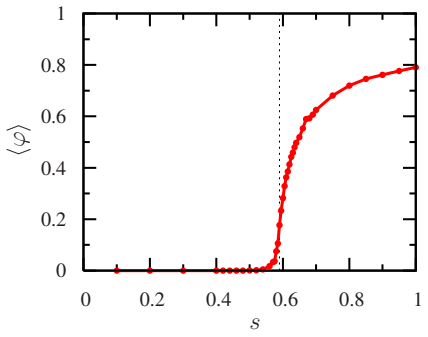

FIG. 1. (Color online) Average velocity $\langle\varphi\rangle$ as a function of the strategy variable s. The data points were obtained by averaging the results of 12 simulations, using the parameters $L=100$, $\rho=0.16$, and $\eta=1/9$, with a relaxation time of $T_{relax}=10\,000$ time steps and averaging over an additional $T_{avr}=10\,000$ time steps.

We characterize the collective motion of particles by the average velocity of all particles φ, defined as

$$\varphi = \frac{1}{N}\left|\sum_{i=1}^{N}\mathbf{v}_i\right|,$$

with N denoting the number of particles in the system. This order parameter can take any value in the range [0,1] and expresses the tendency of particles to move in the same direction. If the particles move randomly, $\varphi=0$, whereas if every particle moves in the same direction, $\varphi=1$. $\langle\varphi\rangle$ was obtained by averaging over 12 individual runs, each recorded after a relaxation time to stationarity T_{relax} and with time averaging over an additional T_{avr} time steps.

III. RESULTS

At first, we investigated the dynamics of the system at different values of the strategy variable s at fixed density and noise values: $\rho=0.16$ and $\eta=1/9$. The density was chosen to be high enough to get flocking, but also tractable in computer simulation. The noise value was a typical value from the ordered state of the original SPP model ($s=1$). We found that by increasing s the system undergoes a phase transition; below a critical value s_c, the ordering, expressed by φ, is negligible, while above s_c the level of order increases rapidly as a function of s (Fig. 1). This is a novel type of phase transition since it corresponds to a phase change *due to a change in the relative strength of a behavioral pattern*.

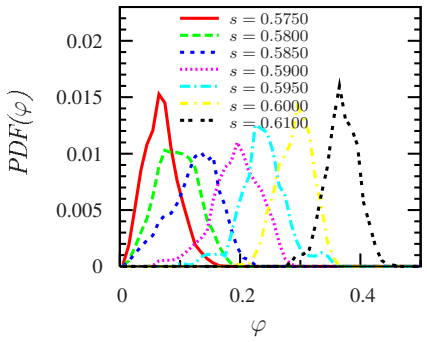

FIG. 2. (Color online) Probability density function (PDF) of the order parameter φ. Parameters as in the previous plot. The one-humped distributions in a range of s values close to the critical one ($s_c \simeq 0.59$) suggest a second-order phase transition.

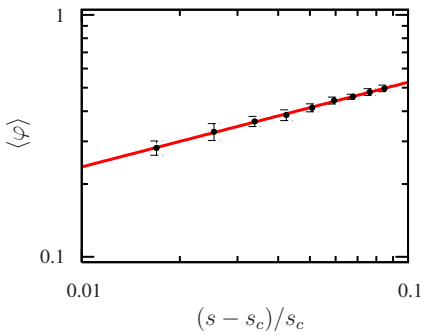

FIG. 4. (Color online) Average velocity values as a function of the distance from the critical point. The fitted line, with $s_c = 0.590 \pm 0.002$, had a slope of $\beta = 0.35 \pm 0.05$. Parameters as in the previous plots.

In order to determine the nature of the phase transition, we also calculated the probability density function (PDF) of φ and the Binder cumulant G at different strategy values. The Binder cumulant, defined as $G = 1 - \langle\varphi^4\rangle / 3\langle\varphi^2\rangle^2$, measures the fluctuations of the order parameter and can be used to distinguish between first- and second-order phase transitions [38]. In case of a first-order phase transition, G exhibits a characteristic minimum, whereas in case of a second-order transition this sharp minimum is absent. In our case the PDF was unimodal, and G did not have a sharp minimum around s_c, both indicating a second-order phase transition (Figs. 2 and 3). G was monotonously increasing, as was observed already in a three-dimensional SNM model with continuous phase transition [34].

Consequently, near the critical point, the order parameter obeys the scaling relation

$$\varphi \sim [s - s_c(\rho, \eta)]^{\beta}, \tag{4}$$

where β is the critical exponent. The critical values s_c and β were determined by plotting $\log\langle\varphi\rangle$ as a function of $\log[(s - s_c)/s_c]$ (Fig. 4). s_c was obtained by finding the value where the plot was the straightest in the relevant region, whereas the critical exponent is equal to the slope of the fitted line. We obtained $s_c = 0.590 \pm 0.002$ and $\beta = 0.35 \pm 0.05$. The value $\beta = 0.35$ is definitely different from 0.5. The latter value would correspond to bifurcation-type instability or to a mean-field solution for which large, nontrivial fluctuations (such as a widely varying size of flocks moving in different directions) at the transition point would not occur. Furthermore, since in the case $s = 1$ (no acceleration term) the simulations resulted in an estimate $\beta = 0.42$ for the behavior of the order parameter as a function of the magnitude of perturbations, we propose that the nature of the transition as a function of the weight of the acceleration term is different (seems to indicate a different universality class) from the transition as a function of the noise.

The critical value of the transition depends on both the density and the noise parameters. Although it needs some careful inspection, Fig. 5 shows that s_c is decreasing with increasing density and increases for increasing noise values.

The order variable φ, by itself, provides a poor description of the two states; hence, we also calculated other statistics. The sinuosity of the particle trajectories was expressed by their average curvature defined as $\lambda = \frac{1}{N}\Sigma_N \frac{|v_i \times a_i|}{|v_i|^3}$.

Two other statistics ψ and μ were used to measure the information exchange between the particles. ψ is defined as the average number of different (formerly not came across)

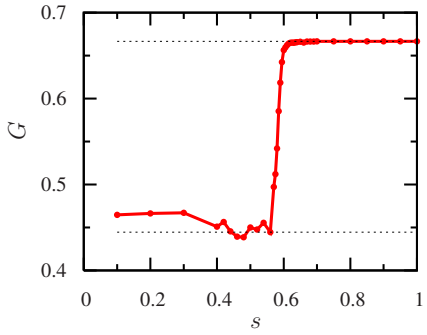

FIG. 3. (Color online) The Binder cumulant G as a function of the strategy variable s. The dotted lines at 2/3 and 4/9 indicate the theoretical value in the case of the ordered and totally disordered states, respectively. Parameters as in the previous plots. The absence of a sharp minimum indicates a second-order phase transition.

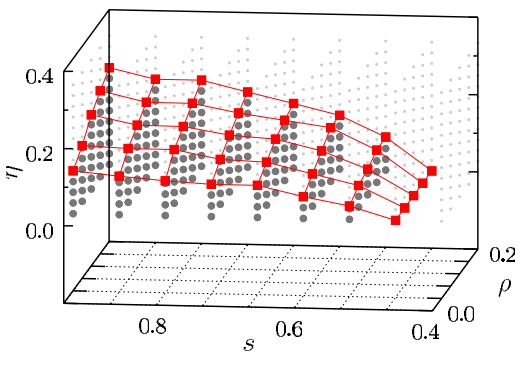

FIG. 5. (Color online) Border surface between the ordered and disordered phases in the s, ρ, η parameter space. The ordered ($\langle\varphi\rangle \geqslant 0.01$) and disordered ($\langle\varphi\rangle < 0.01$) states are indicated by heavy and light dots, respectively. Squares show the critical noise values $\eta_c(s, \rho)$ obtained from the plot of $\log\langle\varphi\rangle$ as a function of $\log[(\eta_c - \eta)/\eta_c]$ for each s and ρ pair. $L = 100$.

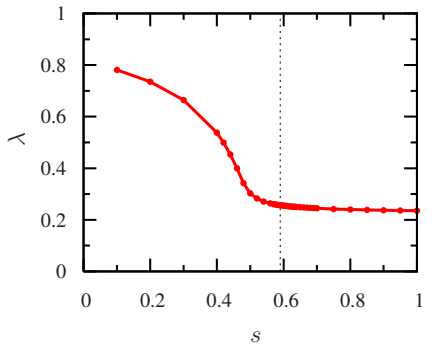

FIG. 6. (Color online) The curvature of trajectories, λ, as a function of the strategy variable s. The dotted line at $s_c=0.590$ indicates the position of the critical point for ordering. Parameters as in the previous plots.

particles encountered—i.e., being within a distance R—by a focal particle during a given time interval. In the simulation we calculated ψ as an average value for 100 initially randomly chosen particles. Although the quantity of ψ depends on the chosen time interval, its monotonicity as a function of s is independent of it. μ was used to evaluate the speed of information propagation as follows. Initially 1% of the particles held the information. The information was transmitted between particles via encounters between information holders and other particles. This way sooner or later every particle became an information holder. μ was defined as the time needed for at least 90% of the particles to become information holders. This aspect of the simulations can also be imagined as tracing of the spread of a disease in a population of flocking units. A more complete version of spreading of an infectious disease in a system of diffusing particles was studied by Gonzalez *et al.* [39].

All three statistics $\langle\lambda\rangle$, $\langle\psi\rangle$, and $\langle\mu\rangle$ were obtained by averaging over 12 individual runs, each after a relaxation time of $T_{relax}=10\,000$ and with an averaging time of $T_{avr}=10\,000$.

The curvature of the trajectories decreases with the strategy variable (Fig. 6). The large curvature at low s values indicates in this case that particles move in small circles (Fig. 7). It is because the large influence of the acceleration term results in continuous turning. This turning is synchronized among neighbors; i.e., their acceleration and velocity vectors become the same, resulting in a particle cloud consisting of separated groups of particles, each containing circling particles. By increasing s the radius of these circles increases, until the circling groups overlap and start to interact with each other. At a critical point the circles overlap so much that neither their position nor their composition remains the same; in other words, the circling groups lose their identity and the particles start to move sinuously. At large s values the movement becomes ordered; all particles tend to move in the same direction, similar to the ordered phase of the SNM model at small velocities.

The dynamics of the system is well reflected in the information propagation (Fig. 8). Both ψ and μ have low values at small s and have a maximum value around s_c. Closely related ideas have been discussed in [40,41]. This result holds for all density and noise parameter values we have investigated. The curves of ψ and μ were very similar, indicating that both are proper measures of information propagation.

In the original SPP model [15] [here, following the notation of Huepe and Aldana [26], called the original Vicsek algorithm (OVA)], the positions of the particles at $t+\Delta t$ depend on two previous time steps t and $t-\Delta t$. In the literature some authors have implemented the model in a slightly dif-

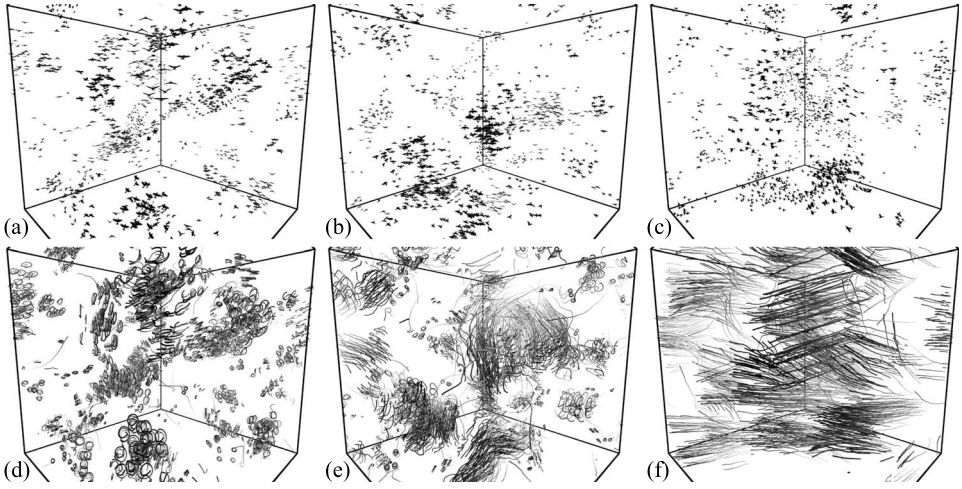

FIG. 7. Shown are the positions and trajectories of particles for different strategy values. These images were obtained by using perspective projection of the three-dimensional data onto two dimensions. This is the view we have if we look at the transparent simulational box with its closest edge being vertical and centered at the observational field. Subfigures show the typical behavior (a), (d) below, (b), (e) near, and (c), (f) above the critical point, respectively. (a)–(c) Positional data of the particles shown as birds. (d)–(f) Each curve shows the trajectory of a particle over 60 time steps after reaching steady state ($t=20\,000$). Different shades of gray indicate the time past, with darker tones denoting more recent positions. (a), (d) Below the critical point, at $s=0.5$, the particles move in circles. (b), (e) Near the critical point, at $s=0.53$, the particles move sinuously. (c), (f) Above the critical point, at $s=0.9$, the particles move in the same direction. $L=20$, $\eta=1/6$, other parameters as in the previous plots.

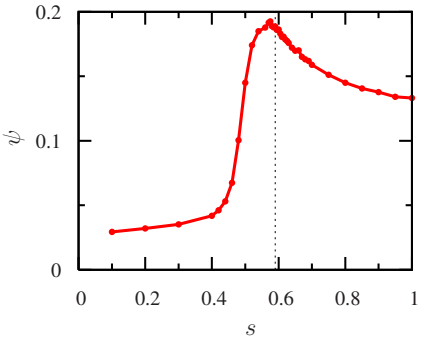

FIG. 8. (Color online) Information exchange between particles (ψ) as a function of the strategy variable s. The curve for μ was very similar (not shown). Parameters as in Fig. 1.

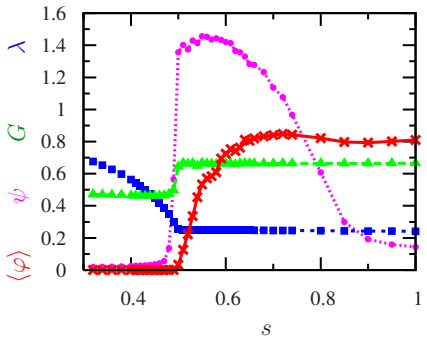

FIG. 9. (Color online) The order parameter ($\langle\varphi\rangle$, × marks), the Binder cumulant (G, triangles), the information exchange between particles (ψ, circles), and the average curvature of trajectories (λ, squares) as a function of the strategy variable s in case of the AC-SPP model with SVA. Compared to the OVA in the case of the SVA, the critical strategy value is at lower s, but the behaviors of the $\langle\varphi\rangle$, G, and λ functions are very similar. The information exchange between particles has its maximum value near the critical point, but it is much more sensible for s. Parameters as in Fig. 1.

ferent way [24,35–37], where the order of the position and the velocity update are changed. Huepe and Aldana [26] refer to this as the standard Vicsek algorithm (SVA), and they report that the local density is different in the OVA and the SVA, while in both cases the average number of interacting neighbors is unreasonably high because of the lack of a repulsive effect. By analyzing the AC-SPP model with an SVA-like updating rule (Fig. 9), we find that the behaviors of the order parameter, the Binder cumulant, and the average curvature are very similar to those in the OVA, but the critical s value is lower. The information exchange rate is, however, rather different, and the maximum value of ψ is much higher in case of the SVA. The maximum value of the information exchange compared to the value at $s=1$ in case of the OVA is $\psi_{max}^{OVA}/\psi_{s=1}^{OVA}=1.4$, while in case of the SVA $\psi_{max}^{SVA}/\psi_{s=1}^{SVA}=10.1$. At $s=1$, where the AC-SPP model is congruous to the original SPP model, the rate of information exchange is similar in the OVA and the SVA.

IV. CONCLUSIONS

In conclusion, we investigated the statistical properties of a three-dimensional self-driven particles system (AC-SPP model) designed to be an improved model for the collective motion of living beings and possibly nonliving units (robots). The ordering of particles exhibited a second-order phase transition as a function of the control parameter corresponding to a behavioral strategy in our case.

We found that the information exchange between particles was maximal at the critical point. Due to the important role of information exchange in animal societies, this might indicate that the critical point corresponds to an optimal behavioral strategy. In a more general context this result suggests that biological evolution may drive individual trait values towards critical ones. However, the validity of this suggestion requires further investigations within an evolutionary game theoretical framework.

ACKNOWLEDGMENTS

This work was supported by EU FP6 grant "Starflag" and by the Hungarian Science Foundation (OTKA), Grant No. 049674.

[1] T. Inagaki, W. Sakamoto, and T. Kuroki, Bull. Jap. Soc. Sci. Fish **42**, 265 (1976).
[2] C. J. Feare, *The Starlings* (Oxford University Press, Oxford, 1984).
[3] E. Ben-Jacob, I. Cohen, O. Shochet, A. Tenenbaum, A. Czirók, and T. Vicsek, Phys. Rev. Lett. **75**, 2899 (1995).
[4] E. M. Rauch, M. M. Millonas, and D. R. Chialvo, Phys. Lett. A **207**, 185 (1995).
[5] J. A. Shapiro, BioEssays **17**, 597 (1995).
[6] J. K. Parrish and L. Edelstein-Keshet, Science **284**, 99 (1999).
[7] B. Szabo, G. J. Szollosi, B. Gonci, Z. Juranyi, D. Selmeczi, and T. Vicsek, Phys. Rev. E **74**, 061908 (2006).
[8] M. Wu, J. W. Roberts, S. Kim, D. L. Koch, and M. P. DeLisa, Appl. Environ. Microbiol. **72**, 4987 (2006).
[9] F. Heppner and U. Grenander, in *The Ubiquity of Chaos*, edited by S. Krasner (AAAS, Washington, 1990), pp. 233–238.
[10] *Animal Groups in Three Dimensions*, edited by J. K. Parrish and W. M. Hamner (Cambridge University Press, Cambridge, England, 1997).
[11] I. D. Couzin and J. Krause, Adv. Study Behav. **32**, 1 (2003).
[12] I. L. Bajec, N. Zimic, and M. Mraz, J. Theor. Biol. **233**, 199 (2005).
[13] I. D. Couzin, J. Krause, N. R. Franks, and S. A. Levin, Nature (London) **433**, 513 (2005).
[14] A. Nathan and V. C. Barbosa, Artif. Life **14**, 179 (2008).
[15] T. Vicsek, A. Czirók, E. Ben-Jacob, I. Cohen, and O. Shochet, Phys. Rev. Lett. **75**, 1226 (1995).
[16] C. W. Reynolds, Comput. Graph. **21**, 25 (1987).
[17] A. Czirók, H. E. Stanley, and T. Vicsek, J. Phys. A **30**, 1375 (1997).

[18] Z. Csahók and T. Vicsek, Phys. Rev. E **52**, 5297 (1995).
[19] J. Toner and Y. Tu, Phys. Rev. Lett. **75**, 4326 (1995).
[20] J. Toner and Y. Tu, Phys. Rev. E **58**, 4828 (1998).
[21] Y. Tu, J. Toner, and M. Ulm, Phys. Rev. Lett. **80**, 4819 (1998).
[22] A. Czirók, M. Vicsek, and T. Vicsek, Physica A **264**, 299 (1999).
[23] G. Grégoire, H. Chaté, and Y. Tu, Phys. Rev. E **64**, 011902 (2001).
[24] G. Grégoire and H. Chaté, Phys. Rev. Lett. **92**, 025702 (2004).
[25] M. Nagy, I. Daruka, and T. Vicsek, Physica A **373**, 445 (2007).
[26] C. Huepe and M. Aldana, Physica A **387**, 2809 (2008).
[27] H. Chaté, F. Ginelli, G. Grégoire, and F. Raynaud, Phys. Rev. E **77**, 046113 (2008).
[28] M. Ballerini, N. Cabibbo, R. Candelier, A. Cavagna, E. Cisbani, I. Giardina, V. Lecomte, A. Orlandi, G. Parisi, A. Procaccini, M. Viale, and V. Zdravkovic, Proc. Natl. Acad. Sci. U.S.A. **105**, 1232 (2008).
[29] J. Gautrais, C. Jost, and G. Theraulaz, Ann. Zool. Fenn. **45**, 415 (2008)
[30] J. Gautrais, C. Jost, M. Soria, A. Campo, S. Motch, R. Fournier, S. Blanco, and G. Theraulaz, J. Math. Biol. (to be published).
[31] F. Heppner, Bird Banding **45**, 160 (1974).
[32] H. Weimerskirch, J. Martin, Y. Clerquin, P. Alexandre, and S. Jiraskova, Nature (London) **413**, 697 (2001).
[33] H. Pomeroy and F. Heppner, Auk **109**, 256 (1992).
[34] B. Gönci, M. Nagy, and T. Vicsek, Eur. Phys. J. Spec. Top. **157**, 53 (2008).
[35] M. Aldana and C. Huepe, J. Stat. Phys. **112**, 135 (2003).
[36] C. Huepe and M. Aldana, Phys. Rev. Lett. **92**, 168701 (2004).
[37] M. Aldana, V. Dossetti, C. Huepe, V. M. Kenkre, and H. Larralde, Phys. Rev. Lett. **98**, 095702 (2007).
[38] K. Binder and D. W. Herrmann, *Monte Carlo Simulation in Statistical Physics: An Introduction* (Springer, Berlin, 1997).
[39] M. C. Gonzalez, P. G. Lind, and H. J. Herrmann, Phys. Rev. Lett. **96**, 088702 (2006).
[40] D. Sumpter, J. Buhl, D. Biro, and I. Couzin, Theory Biosci. **127** , 177 (2008).
[41] R. V. Sole and O. Miramontes, Physica D **80**, 171 (1995).